

# Transient optical elements: application to near-field microscopy

D. SIMANOVSKII, D. PALANKER, K. COHN & T. SMITH

Picosecond Free Electron Laser Center, W.W. Hansen Experimental Physics Laboratory, Stanford University, Stanford, CA 94305-4085, U.S.A.

**Key words.** Fresnel lens, near-field microscopy, transient optical element.

## Summary

We report methods of near-field infrared microscopy with transient optically induced probes. The first technique – a transient aperture (TA) – uses photoinduced reflectivity in semiconductors to generate a relatively large transient mirror (TM) with a small aperture at its centre. We report the optical properties of the TM and TA and experiments performed on near-field imaging with the TA. The second technique is based on solid immersion microscopy, in which high resolution is achieved when light is focused inside a solid with a high refractive index. By creating a transient Fresnel lens on the surface of a semiconductor wafer via photoinduction, we were able to form a solid immersion lens (SIL) for use as a near-field probe. The use of transient probes eliminates the need for mechanical scanning of the lens or sample, and thus provides a much faster scanning rate and the possibility to work with soft and liquid objects.

## Introduction

Scanning near-field microscopy and solid immersion microscopy are well-developed methods of optical imaging that provide spatial resolution beyond the optical diffraction limit. Based on the detection of non-propagating components of an electromagnetic field, near-field microscopy does not have a fundamental limit in spatial resolution. Resolution of about  $\lambda/20$  has been achieved with aperture probes (Dürig *et al.*, 1986; Harootunian *et al.*, 1986; Betzig *et al.*, 1987) and even higher resolution of up to  $\lambda/100$  is available with scattering-type probes (Zenhausern *et al.*, 1994, 1995; Jersch & Dickmann, 1996).

Solid immersion microscopy is an alternative approach to high-resolution imaging, which combines elements of imaging microscopy and probe microscopy. A solid immersion lens (SIL) focuses radiation within a material of a high refractive index, reducing the focal spot diameter by a factor of the refractive index  $n$  in comparison with focusing in vacuum.

With the sample positioned on the flat output surface of the SIL, the microscope is operated in near-field mode using the evanescent field protruding from the SIL into air. SILs can be used as final elements of either imaging or scanning microscopes. The scanning mode of operation allows avoiding aberrations inevitable in imaging regime and thus provides better spatial resolution. In this mode, an SIL can be considered as a near-field probe with very high throughput (Mansfield & Kino, 1990; Wu *et al.*, 1999; Fletcher *et al.*, 2000; Ippolito *et al.*, 2001).

We present two methods of near-field microscopy based upon transient optical elements. These methods have been developed for the mid-infrared range and can be extended to the far-infrared and THz domains. Photoinduced generation of carriers in semiconductors is used to create two- and three-dimensional reflecting and refracting structures. Spatial resolution of these structures is determined by the wavelength of visible light, thus providing confinement of the infrared light on a subwavelength scale.

## Methods

The first technique – a transient aperture (TA) – resembles a fundamental near-field configuration when light is squeezed through a subwavelength aperture in a non-transparent screen. To generate the TA, a subpicosecond laser pulse illuminates a large area of the semiconductor film except for a small region in the middle that is shadowed. In this configuration a large transient mirror (TM) is formed with a small aperture that acts as a near-field probe. We studied the optical properties of the TM and TA and performed experiments on near-field imaging with the TA.

The second technique is based on creating a transient SIL. In order to benefit from using a material with a high refractive index, the focusing element must be incorporated into the material. We used photoinduced reflectivity from a picosecond laser pulse to generate a transient Fresnel lens on the surface of a semiconductor wafer to focus infrared light on the other side of the wafer, where a sample was positioned. Two materials were tested: GaP and Si with refractive indices of 3 and 3.4, respectively. We will discuss such issues as ultimate resolution,

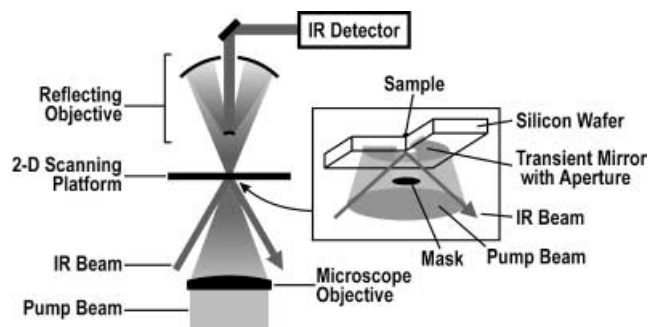


Fig. 1. Experimental set-up for the transient aperture, schematically showing the projection of a mask with the pump beam onto the lower surface of a semiconductor slab using a conventional inverted microscope.

lifetime, contrast parameters, chromatic aberrations and images obtained for this method.

For both methods, the infrared radiation was generated in an optical parametric amplifier (OPA) (Spitfire, Spectra Physics Inc.) pumped by a Ti:S laser (1 mJ, 1 ps, 800 nm, 1 kHz). A fraction (30%) of the Ti:S fundamental was converted to second harmonic and used as a pump beam to generate the photoinduced electron-hole plasma. This wavelength is short enough to provide well-resolved photoinduced structures for mid-IR wavelengths in semiconductors.

To facilitate beam transport, most of the measurements were performed with the IR light at 6.25  $\mu\text{m}$ , owing to the lack of water vapour absorption at this wavelength. IR radiation scattered from the sample positioned on the output surface of the near-field probe was collected with a Cassegrain reflecting objective (Ealing, 25 $\times$ , NA 0.4) and detected with a liquid-nitrogen-cooled mercury-cadmium-telluride (MCT) detector (KMPV-50, Kolmar Technologies).

The general scheme of the TA set-up is shown in Fig. 1. It consists of an XY scanning stage with a sample holder positioned on an inverted optical microscope (Axiovert 35, Karl Zeiss). A slightly diverging pump beam was transmitted through a glass slide with a shadow mask and focused by the microscope objective [Nikon, 503, 0.4 numerical aperture (NA), 13.8 mm working distance] to a 200-mm-diameter circle. The demagnified image (70 $\times$ ) of the mask produced a dark region in the middle of this circle leaving a small opening (TA) in the TM. Different masks were used to produce TAs varying in size from 0.5 to 3  $\mu\text{m}$ . Infrared light was focused by an  $f/10$  focusing system onto the semiconductor surface at a grazing angle of 20°. At this angle no direct light was collected by the reflecting objective, so only scattered radiation reached the MCT detector.

## Results and discussion

While the second harmonic of the Ti:S laser light can be used to induce strong photorefectivity in many semiconductor

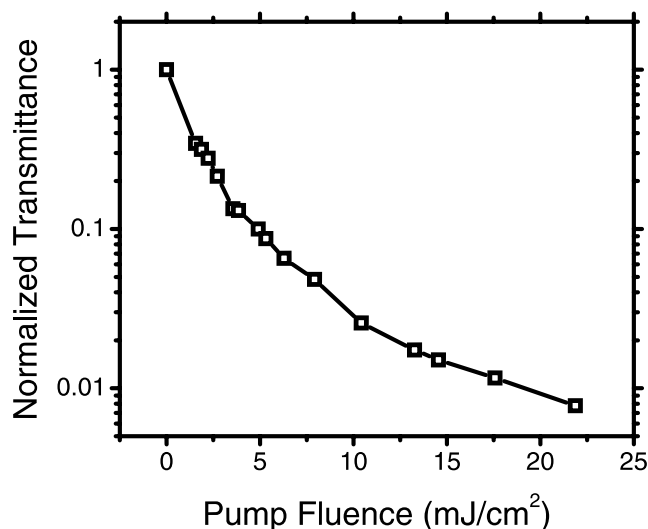


Fig. 2. Transmittance of photoexcited Si at 6.25  $\mu\text{m}$  as a function of pump fluence at 400 nm.

materials, one of the best is silicon, since it has a high damage threshold for 400-nm irradiation ( $\sim 20 \text{ mJ cm}^{-2}$ ) and a shallow penetration depth (80 nm). Transmittance of bulk Si was measured as the function of pump light fluence and is shown in Fig. 2. The decreasing transmittance is a combination of reflection and absorption, and sets requirements on the contrast of the shadow mask image. A saturated TM with a highly transparent TA can be created if the pump light intensity in the shadow region is less than 10% of that in the illuminated area.

The pump light intensity distribution in the microscope focal plane was measured directly with an optical probe. A 0.3- $\mu\text{m}$ -diameter hole in a 100-nm-thick metal screen was scanned in the focal plane, and light transmitted through this hole was detected by a photodiode. The contrast ratio of the image of a 1- $\mu\text{m}$  mask was found to be better than 100 and the edge sharpness was better than 0.5  $\mu\text{m}$ . These results are consistent with the diffraction-limited resolution of the objective used. Results of the transmission measurements are presented in Fig. 3. Line 1 shows the signal recorded when the semiconductor surface was illuminated through the shadow mask. This signal consists of the light transmitted through the aperture and the background signal, which we believe results from light scattered from inhomogeneities in the TM. Precise alignment of the IR collecting objective helped to reduce the field of view of the detection system and thus the background radiation. The minimum size of the field of view is set by the diffraction limit and was equal to 10  $\mu\text{m}$ . Line 2 of Fig. 3 represents the background signal recorded at the illumination geometry, but without the mask. At high pump intensities the background level is reduced and the signal background ratio for the 1- $\mu\text{m}$  aperture exceeds 100.

As a test object for imaging we used a set of 1.7- $\mu\text{m}$ -diameter holes in a 200-nm-thick gold film on an Si wafer.

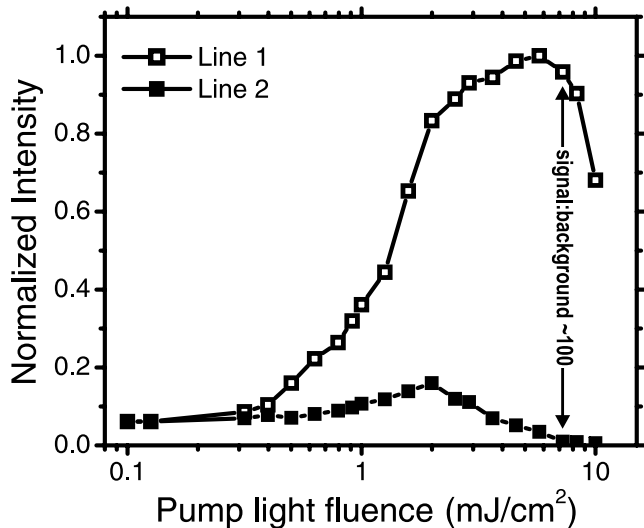


Fig. 3. Transmission of the 1- $\mu\text{m}$  transient aperture at 6.25  $\mu\text{m}$  as a function of pump light fluence.

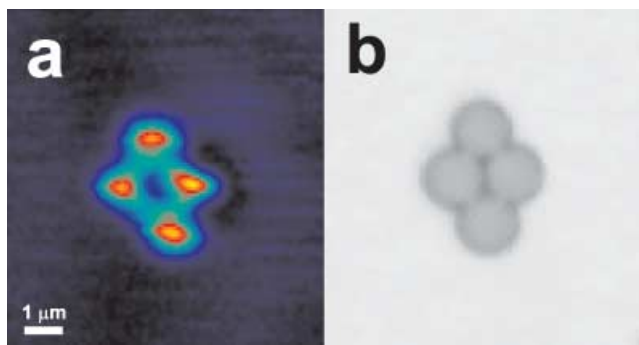


Fig. 4. Images of the four-hole structure in a gold film. (a) Near-field IR image; (b) visible light image obtained with a conventional microscope.

This structure was prepared by depositing micrometre-sized polystyrene beads on Si, coating it with gold, and then flushing the polystyrene beads away. The Si wafer with the sample structure was raster scanned in the focal plane common for both the illuminating and the detecting systems. With a 1-kHz repetition rate laser system, scanning time was typically 15 s, providing images with  $128 \times 128$  resolution. Figure 4(a) shows an IR image taken with the TA of four adjacent 1.7- $\mu\text{m}$ -diameter holes, and for comparison Fig. 4(b) shows the holes imaged optically. These holes are completely resolved, and demonstrate a resolution of better than  $\lambda/5$ .

One problem with the TA technique is that it typically requires semiconductor substrates no thicker than 1 or 2  $\mu\text{m}$ . These substrates are extremely brittle and difficult to manufacture. Our second method circumvents this problem with a diffractive optical element (DOE) generated on the surface of semiconductors, and particularly a DOE-SIL, utilizing the remarkably high refractive indices characteristic of many

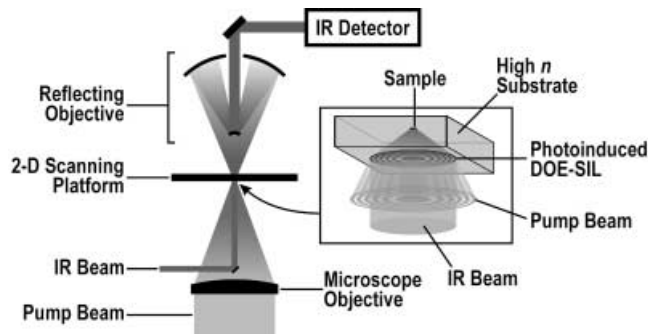


Fig. 5. Experimental set-up for the DOE-SIL. The infrared light focused by a transient SIL inside the semiconductor is collected after propagation through the sample located on the upper surface of the slab.

semiconductors. These elements are much more versatile in comparison with simple aperture probes, and they do not require thin semiconductor substrates. The simplest DOE-SIL is a Fresnel lens drawn on one side of a flat semiconductor wafer with its focus on the other side. As was the case for the aperture, the fact that the SIL can be created in a transient manner allows for remarkable easy scanning, by raster scanning the wafer in the focal plane of the optical system while redrawing the DOE for each wafer position.

To create the transient DOE-SIL, a 70-fold demagnified image of a lithographic mask with blocked and opened zones was projected onto the surface of the semiconductor with the second harmonic of the Ti:S laser. Illuminated regions of the semiconductor became opaque to the IR light and thus worked as 'dark' zones, while shadowed areas remained transparent and worked as 'opened' zones. Elements of the projection system and IR optics are presented in Fig. 5.

The two semiconductor wafers used in our experiment were 300- $\mu\text{m}$ -thick GaP and 28- $\mu\text{m}$ -thick Si. Fresnel lenses were designed for both to have a numerical aperture (NA) of about two. Lens diameters of 450 and 60  $\mu\text{m}$  – corresponding to 70 and 15 zones – were required to achieve such an NA on GaP and Si, respectively. The Fresnel lenses were illuminated with a nearly parallel 600- $\mu\text{m}$ -diameter IR beam directed normally to the wafer by a small mirror.

Figure 6 shows images of a single 1.8- $\mu\text{m}$  hole obtained with the GaP DOE-SIL (a) and Si DOE-SIL (b). Both spot sizes represent a convolution of the actual intensity distribution in the focal plane with the hole size. Since the hole size is not larger than the expected focal spot size and the convolution algorithm for a near-field interaction is strongly non-linear, we assume that the experimental lines are close to the actual spot profile.

The two tested DOE-SILs with comparable NAs should have provided similar results; however, they did not. One can see from Fig. 6 that in our case, the 15-zone lens on Si performs better than 70-zone lens on GaP. This is not unexpected because elements with larger diameters are more sensitive to

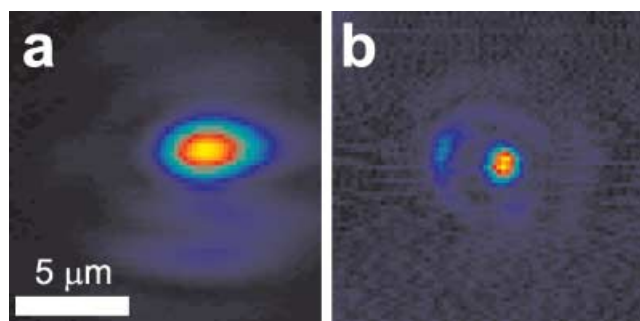


Fig. 6. The IR images of a 1.8- $\mu\text{m}$  hole imaged with the GaP DOE-SIL (a), and the Si DOE-SIL (b).

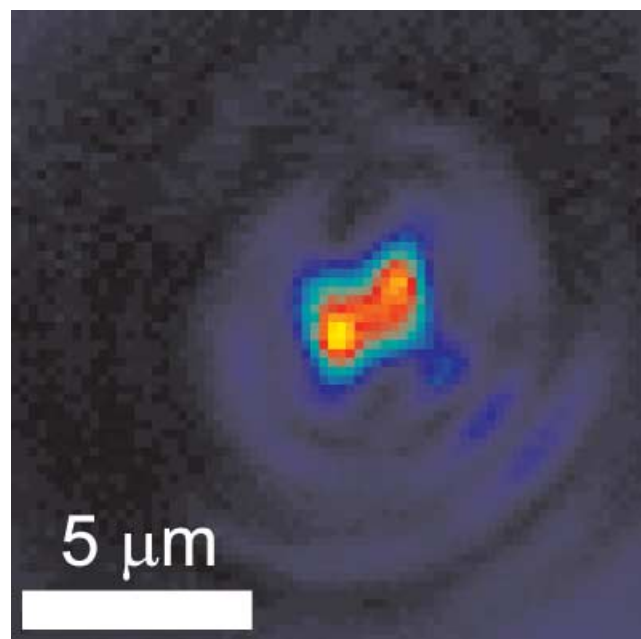


Fig. 7. The IR image of two 1.8- $\mu\text{m}$ -diameter touching holes obtained with the Si DOE-SIL.

any irregularities in the structure periodicity resulting from the imperfections of the projection system, and – more importantly in our case – they introduce longer delays between IR light travelling from the central and outer zones. This delay is comparable to the IR pulse duration and hinders constructive interference of light scattered from different zones. Furthermore, the spectral bandwidth of the DOE-SIL becomes narrower by increasing the number of zones, giving rise to chromatic aberrations.

Since the thinner lens showed superior focusing properties in comparison with the thicker one, the 28- $\mu\text{m}$ -thick Si-based lens was chosen for further study. To demonstrate the ability to resolve more complex objects, an image of two touching 1.8- $\mu\text{m}$  holes was taken (Fig. 7), with the two holes easily discernible.

The focusing characteristics and contrast of transient DOE-SILs can be further improved by using advanced diffractive structures. Among them are structures with gradually modulated absorbance, structures utilizing foci of different orders, and, probably most importantly, structures employing phase modulation. Phase modulation, which requires modification of the refractive index over significant depth, can be achieved in semiconductors using pump radiation with a long penetration depth. Such techniques might be used to create three-dimensional structures with possible applications ranging from the focusing of light to creating complex photonic crystals used for signal processing.

The initial results of near-field microscopy with transient elements demonstrate that photoinduction in semiconductors can be used to create near-field probes for mid-IR radiation. Resolution of about 1  $\mu\text{m}$  ( $> \lambda/5$ ) was demonstrated with the TA, and similar resolution was shown with the DOE-SIL. Both techniques eliminate the need for the mechanical scanning of the lens or sample.

#### Acknowledgements

This work was funded by the National Science Foundation (#DBI-9819778) and by the Department of the Air Force (#F49620-00-1-0349).

#### References

- Betzig, E., Isaacson, M. & Lewis, A. (1987) Collection mode near-field scanning optical microscopy. *Appl. Phys. Lett.* **51**, 2088–2090.
- Dürig, U., Pohl, D.W. & Rohner, F. (1986) Near-field optical-scanning microscopy. *J. Appl. Phys.* **59**, 3318–3327.
- Fletcher, D.A., Crozier, K.B., Quate, C.F., Kino, G.S., Goodson, K.E., Simanovskii, D. & Palanker, D.V. (2000) Near-field infrared imaging with a microfabricated solid immersion lens. *Appl. Phys. Lett.* **77**, 2109–2111.
- Harootunian, A., Betzig, E., Isaacson, M. & Lewis, A. (1986) Super-resolution fluorescence near-field scanning optical microscopy. *Appl. Phys. Lett.* **49**, 674–676.
- Ippolito, S.B., Goldberg, B.B. & Ünlü, M.S. (2001) High spatial resolution subsurface microscopy. *Appl. Phys. Lett.* **78**, 4071–4073.
- Jersch, J. & Dickmann, K. (1996) Nanostructure fabrication using laser field enhancement in the near field of a scanning tunneling microscope tip. *Appl. Phys. Lett.* **68**, 868–870.
- Mansfield, S.M. & Kino, G.S. (1990) Solid Immersion Microscopy. *Appl. Phys. Lett.* **57**, 2615–2616.
- Wu, Qiang, Feke, G.D., Grober, Robert, D. & Ghislain, L.P. (1999) Realization of numerical aperture 2.0 using a gallium phosphide solid immersion lens. *Appl. Phys. Lett.* **75**, 4064–4066.
- Zenhausern, F., Martin, Y. & Wickramasinghe, H.K. (1995) Scanning interferometric apertureless microscopy: optical imaging at 10 angstrom resolution. *Science*, **269**, 1083–1085.
- Zenhausern, F., O'Boyle, M.P. & Wickramasinghe, H.K. (1994) Apertureless near-field optical microscope. *Appl. Phys. Lett.* **65**, 1623–1625.